Dent Mater 12:333-341, November, 1996

X-ray diffraction studies of oxidized high-palladium alloys

William A. Brantley[1], Zhuo Cai[2,3], Efstratios Papazoglou[1], John C. Mitchell[4], Susan J. Kerber[5], Gregory P. Mann[6], Tery L. Barr[6]

[1]*Section of Restorative Dentistry, Prosthodontics and Endodontics, College of Dentistry,*
[2]*Section of Oral Biology, College of Dentistry,*
[3]*(Now at The Texas A & M University System, Baylor College of Dentistry, Dallas, Texas, USA)*
[4]*Microscopic and Chemical Analysis Research Center (MARC),*
Department of Geological Sciences, The Ohio State University, Columbus, Ohio, USA
[5]*Material Interface, Inc., Sussex, Wisconsin, USA*
[6]*Department of Materials, Laboratory for Surface Studies, University of Wisconsin-Milwaukee, Milwaukee, Wisconsin, USA*

ABSTRACT

Objective. The purpose of this study was to use x-ray diffraction (XRD) to obtain new information about the oxide layers on four representative oxidized high-palladium alloys.

Methods. Cast specimens of two Pd-Cu-Ga alloys and two Pd-Ga alloys, with both polished and etched surfaces and air-abraded surfaces, were subjected to oxidation procedures recommended by the manufacturers. The specimens were analyzed by x-ray diffraction using CuKα radiation, and the peaks were compared to appropriate Joint Committee on Powder Diffraction Standards (JCPDS).

Results. The surface preparation procedure had a profound effect on the phases present in the oxide layers. For the specimens that had been polished and etched, $CuGa_2O_4$ and β-Ga_2O_3 were detected on the 79Pd-10Cu-9Ga-2Au alloy, whereas SnO_2 and $CuGa_2O_4$ were detected on the 76Pd-10Cu-5.5Ga-6Sn-2Au alloy. The oxide layers on both Pd-Cu-Ga alloys contained Cu_2O, and the oxide layer on the 76Pd-10Cu-5.5Ga-6Sn-2Au alloy may contain β-Ga_2O_3. The principal phase in the oxide layers on both Pd-Ga alloys that had been polished and etched was In_2O_3, which exhibited extreme preferred orientation. No other phase was detected in the oxide layer on the 85Pd-10Ga-2Au-1Ag-1In alloy, whereas β-Ga_2O_3 was found in the oxide layer on the 75Pd-6Ga-6Au-6Ag-6.5In alloy. For the air-abraded specimens, β-Ga_2O_3 was not present in the oxide layers on the Pd-Cu-Ga alloys, and β-Ga_2O_3 was the major phase in the oxide layers on the Pd-Ga alloys. Palladium oxide(s) in varying amounts were detected for both surface preparations of the Pd-Cu-Ga alloys and for the air-abraded Pd-Ga alloys. Except for the 76Pd-10Cu-5.5Ga-6Sn-2Au alloy, the oxide layer caused minimal change in the lattice parameter of the palladium solid solution compared to that for the as-cast alloy.

Significance. Knowledge of the phases found in the oxide layers on these high-palladium alloys is of fundamental importance for interpreting differences in the adherence of dental porcelain to the metal substrates under static and dynamic conditions, and may provide guidance in the development of new high-palladium alloys with improved metal-ceramic bonding.

INTRODUCTION

It is well-known that adherence between dental porcelain and the alloy substrate generally depends upon development of strong chemical bonds across the interface through an oxide layer on the alloy, as well as upon mechanical interlocking at microirregularities created on the alloy surface by air abrasion (Philips, 1991; Craig, 1993). While occasionally a dental alloy may not form an external oxide (Mackert *et al.*, 1983) and porcelain adherence must be achieved through mechanical retention, Mackert *et al.* (1988) have shown that there is a direct relationship between oxide adherence and metal-ceramic bonding for alloys forming external oxides.

Although high-palladium dental alloys containing greater than about 75 wt% Pd have become popular for metal-ceramic restorations over the past decade because of their lower cost than gold alloys and their good mechanical properties (Carr and Brantley, 1991; Brantley *et al.*, 1993), only limited information is available about their oxidation behavior. Cascone (1983) reported that both Ga_2O_3 and CuO external oxides, along with a CuO internal oxide, formed during simulated porcelain firing heat treatment for model Pd-Cu-Ga alloys, and the two surface oxides reacted to form $CuGa_2O_4$ spinel. Using x-ray diffraction (XRD), Hautaniemi *et al.* (1990) identified $CuGa_2O_4$ on the surface of an oxidized Pd-Cu-Ga alloy with a composition very similar to that of Option (J. M. Ney Company, Bloomfield, CT, USA) and Spartan (Williams Division, Ivoclar North America, Amherst, NY, USA). Bagby *et al.* (1990) also employed XRD to identify SnO_2 and $CuGa_2O_4$ on another oxidized Pd-Cu-Ga alloy (Deguplus 2, Degussa Dental, Inc., South Plainfield, NJ, USA). Using an indirect approach, van der Zel (1989) employed measurements of alloy weight changes during oxidation and emission spectroscopic analyses of HCl leaching solutions to deduce the phases originally present in the oxide layers. The compositions of subsurface oxides were determined by x-ray energy-dispersive spectroscopic analyses with the scanning electron microscope (SEM/EDS).

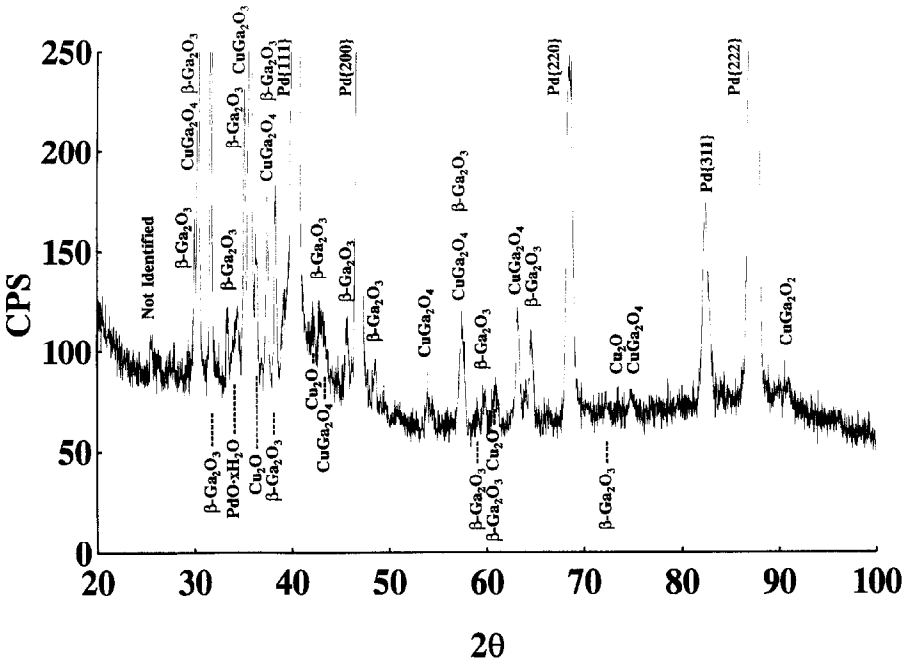

Fig. 1. **X-ray diffraction pattern obtained with the Scintag PAD-V diffractometer for oxidized, polished and etched Pd-Cu-Ga alloy Spartan Plus.**

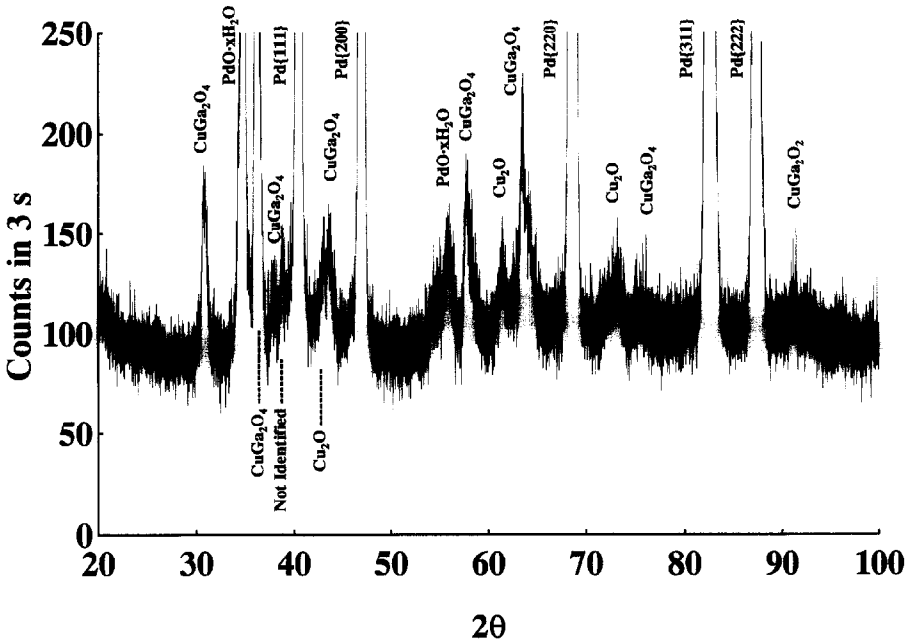

Fig. 2. **X-ray diffraction pattern obtained with the Philips diffractometer for oxidized air-abraded Pd-Cu-Ga alloy Spartan Plus.**

Using experimental techniques developed by Ringle *et al.* (1983) and Mackert *et al.* (1988), Papazoglou *et al.* (1993) measured the adherence of Vita VMK dental porcelain (Vident, Baldwin Park, CA, USA) to four high-palladium alloys after debonding the porcelain in biaxial flexure. It was found that the porcelain adherence was significantly greater for the two Pd-Cu-Ga alloys (Spartan Plus, Williams/Ivoclar; Liberty, J.F. Jelenko & Company, Armonk, NY, USA), compared to the two Pd-Ga alloys (Protocol, Williams/Ivoclar; Legacy, Jelenko). The purpose of this investigation was to use XRD to obtain detailed information about the phases present in the oxidized layers on these four alloys. No studies of the oxidation behavior of the Pd-Ga alloys have previously been reported. XRD analyses of the four high-palladium alloys in the as-cast condition were recently published (Brantley *et al.*, 1995).

MATERIALS AND METHODS

The Pd-Cu-Ga alloys selected for study (Spartan Plus, Williams/Ivoclar and Liberty, Jelenko) had compositions of 79Pd-10Cu-9Ga–2Au and 76Pd-10Cu-5.5Ga–6Sn-2Au, respectively, whereas the Pd-Ga alloys (Protocol, Williams/Ivoclar and Legacy, Jelenko) had compositions of 75Pd-6Ga–6Au-6Ag-6.5In and 85Pd-10Ga–2Au-1Ag-1In, respectively (Brantley *et al.*, 1995). The composition of the Spartan Plus alloy is identical to that of the previously mentioned Option and Spartan alloys, except for the absence of a small amount of boron (Brantley *et al.*, 1995).

Two types of oxidized specimens were prepared for each alloy. One cast specimen, 20 mm x 20 mm x 1.5 mm, used in the previous XRD investigation of the as-cast structure (Brantley *et al.*, 1995), was metallographically polished through 0.05 μm alumina slurries, etched in aqua regia solutions (Mezger *et al.*, 1988) and subjected to the initial oxidation procedure recommended by the manufacturer. These specimens were polished and etched prior to oxidation in order to have a reproducible level of surface roughness with minimal residual plastic deformation. Although recommended by the manufacturer, no subsequent air abrasion was performed on the two oxidized Jelenko (Liberty and Legacy) alloys. A second cast specimen of smaller dimensions, 10 mm x 10 mm x 1 mm, was air-abraded, following standard dental laboratory practice, and subjected to the same recommended oxidation procedure. A smaller size was used for the oxidized air-abraded specimens so that they could be used for further study.

The two Williams/Ivoclar alloys (Spartan Plus and Protocol) were oxidized by heating in vacuum in a conventional dental porcelain furnace from 650° to 1,010°C at a rate of 56°C per min with a 5 min hold at the peak temperature, whereas the two Jelenko alloys (Liberty and Legacy) were oxidized by heating in air from 704° to 1,010°C at 56°C per min with no hold at the peak temperature.

The XRD patterns for all oxidized specimens were obtained at room temperature, using CuKα radiation (λ = 1.54060 Å). The oxidized, polished and etched specimens were analyzed by an x-ray diffractometer (PAD-V, Scintag, Sunnyvale, CA, USA) with a nickel filter, operating over a 2θ range from 20°-100°

TABLE 1 SUMMARY OF X-RAY DIFFRACTION PEAKS FOR OXIDIZED AIR ABRADED SPARTAN PLUS

184	30.77	2.904	$CuGa_2O_4$ (2.934 and 30) Poor match
430	34.78	2.577	$PdO \cdot xH_2O$ (2.615 and 100) Poor match to JCPDS standard Identification based upon XPS results
358	36.05	2.490	$CuGa_2O_4$ (2.502 and 100)
135	37.96 (avg.)*	2.369	$CuGa_2O_4$ (2.395 and 12) Poor match because of peak breadth
155	38.81	2.319	Not identified
5,307	40.53	—	111 Palladium solid solution
159	43.07	2.098	Cu_2O (2.135 and 37) Poor match Shifted by adjacent $CuGa_2O_4$ peak
165	43.59	2.075	$CuGa_2O_4$ (2.074 and 17)
1,820	47.01	—	200 Palladium solid solution
125	53.98	1.697	$CuGa_2O_4$ (1.694 and 10)
138	54.76	1.675	Cu_2O (1.668 and 60)
165	55.97	1.642	$PdO \cdot xH_2O$ (1.668 and 60). Similar discrepancy with standard as peak at 34.78°.
190	57.73	1.596	$CuGa_2O_4$ (1.597 and 35)
146	61.46	1.507	Cu_2O (1.510 and 27)
230	63.63	1.461	$CuGa_2O_4$ (1.467 and 40)
1,034	68.68	—	220 Palladium solid solution
158	73.30	1.290	Cu_2O (1.287 and 17)
140	75.22	1.262	$CuGa_2O_4$ (1.265 and 8)
862	82.81	—	311 Palladium solid solution
434	87.55	—	222 Palladium solid solution
152	91.50	1.075	$CuGa_2O_4$ (1.080 and 12)

at a continuous scanning rate of 0.5° per min and a photon-counting interval of 0.03°. The oxidized air-abraded specimens were analyzed with two x-ray diffractometers. A high-precision wide-range goniometer (Philips Electronics PW 1316/90, Philips, Eindhoven, The Netherlands) with XRG 3100 x-ray generator, DMS-41 measuring system and graphite monochromator was operated over a 2θ range from 20°-100° at step intervals of 0.01° and a photon-counting time of 3 s per step. In addition, x-ray diffraction patterns were obtained over the narrower 2θ range of 20°-70° to confirm the locations of the peaks from the oxides, using a Scintag Model 2000 XRD system with a solid state analysis filter. These scans were performed at 2θ steps of 0.030° and photon-counting times of 0.36 s (Spartan Plus) or 0.45 s (Liberty, Legacy and Protocol) per step. The smaller oxidized air-abraded specimens were mounted on a silicon single crystal substrate having a special orientation which did not yield significant diffraction peaks.

The peaks for the oxide layers were indexed to the JCPDS (Joint Committee on Powder Diffraction Standards, Swarthmore, PA, USA) file of pure polycrystalline powder standards. The Nelson-Riley analysis (Cullity, 1978) was employed with linear regression to determine the lattice parameter of the palladium solid solution in the four oxidized alloys from the positions of the 111, 200, 220, 311 and 222 peaks. Accuracy of the results obtained with the Scintag PAD-V diffractometer was validated by agreement of the lattice parameter of the palladium solid solution for one as-cast alloy (Legacy) serving as a control within 0.01 Å of the value previously determined (Brantley *et al.*, 1995) with the Philips diffractometer, which was periodically calibrated with crystallographic standards. Accuracy of the results obtained with the Scintag Model 2000 diffractometer was validated by comparison of the lattice parameter of the palladium solid solution in the oxidized alloys and the positions of the peaks from the oxides with values obtained with the Philips diffractometer; these values generally agreed within 0.01 Å.

RESULTS

The x-ray diffraction pattern for the oxidized, polished and etched 79Pd-10Cu-9Ga-2Au alloy Spartan Plus is shown in Fig. 1. The diffracted x-ray intensity obtained during continuous scanning with the Scintag PAD-V diffractometer is given in terms of counts per second (cps). Each peak has been labeled with the corresponding phase(s); there are four peaks that may correspond to overlapping peaks from two different phases. The phases detected in the oxide layer were $CuGa_2O_4$ (standard 26-514), β-Ga_2O_3 (standard 41-1103), Cu_2O (standard 5-667), and possibly hydrated palladium oxide ($PdO \cdot xH_2O$) (standard 9-254). The matches of the peak positions with those predicted from the four JCPDS standards using CuKα radiation were excellent, as corresponding values for interplanar spacings (d-spacings) were generally within 0.01 Å for all peaks from each phase. Comparisons of predicted peak positions for α-Ga_2O_3 (standard 41-1103), CuO (standard 41-524), and PdO (standard 41-1107) with peaks for the oxide layer indicated that these phases were not present.

The x-ray diffraction pattern in Fig. 2 shows that the oxide layer on air-abraded Spartan Plus consisted of $CuGa_2O_4$, Cu_2O, and perhaps both $PdO \cdot xH_2O$ and PdO. The diffracted x-ray intensity obtained with the Philips diffractometer is given in terms of counts per 3 s, the time interval for each step during scanning. The peak positions and their interpretation have been summarized in Table 1. In contrast to the oxidized, polished and etched specimen in Fig. 1, no β-Ga_2O_3 was present. There was similar excellent agreement for all of the $CuGa_2O_4$ and Cu_2O peaks with the d-spacings in the JCPDS standards, except for the $CuGa_2O_4$ peak at 30.77° where there was a discrepancy of 0.03 Å, and the Cu_2O peak at 43.07° where there was overlap with an adjacent $CuGa_2O_4$ peak. Assignment of the strongest oxide peak at 34.78° to $PdO \cdot xH_2O$ was based upon x-ray photoelectron spectroscopic (XPS) analysis of a nominally identical specimen, although the d-spacings for the two peaks indexed to this oxide were 0.03 Å to 0.04 Å less than those for the JCPDS standard. A peak corresponding to the strongest peak for PdO at d = 2.647 Å was

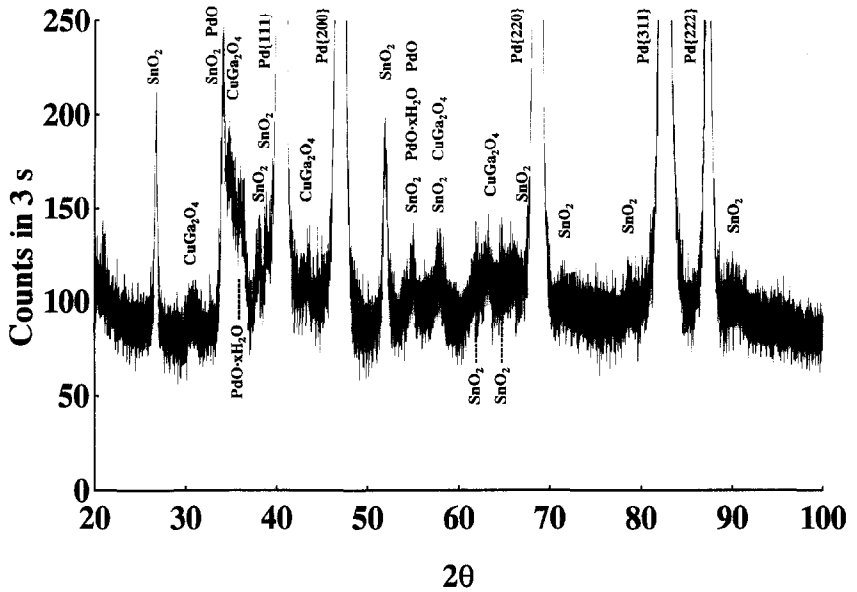

Fig. 3. **X-ray diffraction pattern obtained with the Philips diffractometer for oxidized air-abraded Pd-Cu-Ga alloy Liberty.**

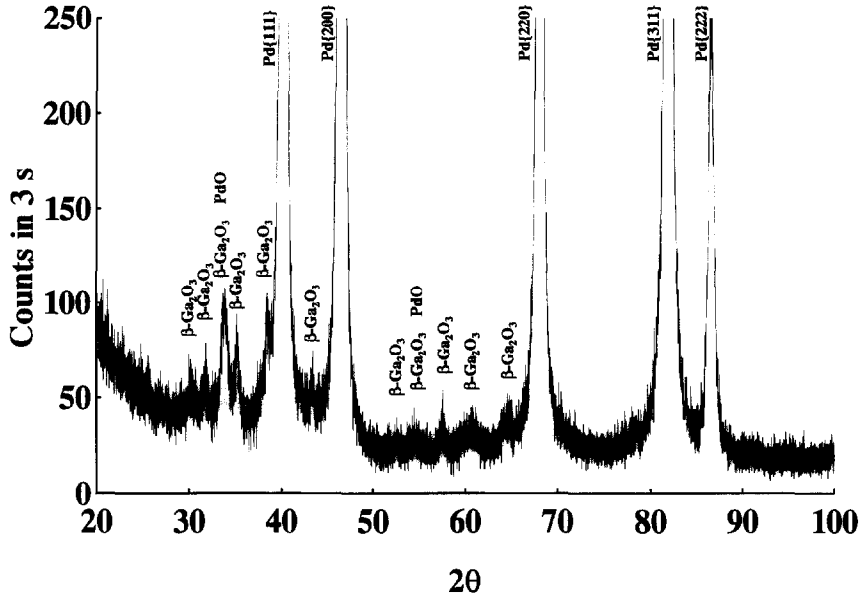

Fig. 4. **X-ray diffraction pattern obtained with the Philips diffractometer for oxidized air-abraded Pd-Cu-Ga alloy Legacy.**

detected with the Scintag Model 2000 diffractometer, but was not evident in the detailed (2θ, Intensity) data for Fig. 2.

Analysis of the x-ray diffraction pattern for the oxidized, polished and etched 76Pd-10Cu-5.5Ga–6Sn-2Au alloy Liberty indicated that the principal phases in the oxide layer were SnO_2, $CuGa_2O_4$ and Cu_2O; β-Ga_2O_3 and PdO·xH_2O also appeared to be present. Other than the strongest peak for SnO_2 (standard 41-1445) where there was a difference of 0.02 Å, the calculated d-spacings of peaks observed for the oxide layer were within 0.01 Å of values given for the SnO_2, $CuGa_2O_4$ and Cu_2O standards. All peaks for the $CuGa_2O_4$ standard were detected, as were all peaks for the SnO_2 standard with relative intensities > 4 except for the peak at d = 1.154 Å, which was obsured by the 311 peak for the palladium solid solution; the three strongest peaks for the Cu_2O standard were also detected. A peak at 34.85°, located between much stronger peaks for SnO_2 and $CuGa_2O_4$, suggested the presence of β-Ga_2O_3 and PdO·xH_2O although the matches of the d-spacings to the JCPDS standards were poor (differences of 0.02 Å and 0.04 Å, respectively). Since the other strong peaks for β-Ga_2O_3 were obscured by peaks for $CuGa_2O_4$ and SnO_2, there was some uncertainty about the presence of β-Ga_2O_3. Moreover, while six of the seven strongest peaks for α-Ga_2O_3 lie at nearly the same positions as peaks for SnO_2 and $CuGa_2O_4$, the absence of the d = 1.815 Å peak for the JCPDS standard suggested that α-Ga_2O_3 was not present in the oxide layer. Comparison of observed peak positions with JCPDS 41-524 indicated that CuO was not present.

The x-ray diffraction pattern for oxidized air-abraded Liberty (Fig. 3) and the analysis of the XRD peaks detected with the Philips diffractometer (Table 2) show that the major phase in the oxide layer was SnO_2. The interplanar spacings agreed within 0.01 Å of the JCPDS values, except for the strongest peak at 26.76° where the discrepancy was 0.02 Å. Four of the five strongest peaks from the JCPDS for $CuGa_2O_4$ were present, and there was excellent agreement of the d-spacings within 0.01 Å of the values from the JCPDS. However, there was poor agreement for the broad $CuGa_2O_4$ peak at 30.99°, where the d-spacing was 0.05 Å less than that from the JCPDS. Palladium oxide(s) also appeared to be present in the oxide layer. The match of the peak at 34.82° to the strongest PdO·xH_2O peak may be poor because the peak position has been additionally shifted by the adjacent SnO_2 peak, and another peak for PdO·xH_2O may be a component of the SnO_2 peak at 54.92°; the PdO·xH_2O peak at d = 1.303 Å was not detected. While the strongest peaks for Cu_2O were not observed, the presence of PdO could not be ruled out because the strongest peaks nearly coincide with SnO_2 peaks. Definitive conclusions about the palladium oxide species in this oxide layer and the presence of Cu_2O will require XPS analyses, which are in progress for this alloy.

Table 3 presents the x-ray diffraction pattern for the oxidized, polished and etched 85Pd-10Ga–2Au-1Ag-1In alloy Legacy. All peaks other than those for the alloy substrate have been indexed to body-centered cubic (bcc) In_2O_3 (standard 6-416). All of the strongest peaks for β-Ga_2O_3 and α-Ga_2O_3 were missing; the α-Ga_2O_3 peak at d = 2.491 Å is nearly coincident with the In_2O_3 peak at d = 2.483 Å. Comparisons of the peak positions in Table 3 with the JCPDS indicated that none of the silver and palladium oxides were present, nor were any of the $(Ga,In)_2O_3$, β-$GaInO_3$, $AgGaO_2$, $AgInO_2$ mixed oxides. Table 3 shows that the In_2O_3 phase had an extremely high degree of preferred orientation. The intensity of the strongest In_2O_3 peak at 22.04° (d = 4.030 Å) was 1,947 cps (counts per second), which was greater than that of the 200 peak for the palladium solid solution matrix of the substrate at 46.73° (1,190 cps); the maximum intensity for the 111 peak of the palladium solid solution at 40.16° was 6,870 cps. The strongest In_2O_3 peak in Table 3 corresponds to the 211 reflection, which is only the fifth-strongest peak for the

TABLE 3. SUMMARY OF X-RAY DIFFRACTION PEAKS FOR OXIDIZED AIR-ABRADED LIBERTY

212	26.76	3.329	SnO_2 (3.347 and 100) Poor match to JCPDS
112	30.99 (avg.)	2.883	$CuGa_2O_4$ (2.934 and 30) Poor match
253	34.01	2.634	PdO (2.647 and 100) SnO_2 (2.643 and 75)
200	34.82	2.574	$PdO \cdot xH_2O$ (2.615 and 100) Poor match
166	35.73 (avg.)	2.511	$CuGa_2O_4$ (2.502 and 100)
146	38.10 (avg.)	2.360	SnO_2 (2.369 and 21)
153	39.17 (avg.)	2.298	SnO_2 (2.309 and 4) Indicates preferred orientation
3,375	40.52	—	111 Palladium solid solution
131	43.51	2.078	$CuGa_2O_4$ (2.074 and 17)
986	47.02	—	200 Palladium solid solution
209	51.93	1.759	SnO_2 (1.764 and 57)
136	54.92 (avg.)	1.671	SnO_2 (1.675 and 14) PdO (1.676 and 20) $PdO \cdot xH_2O$ (1.668 and 60)
140	57.61	1.599	$CuGa_2O_4$ (1.597 and 35) SnO_2 (1.593 and 6)
143	62.02 (avg.)	1.495	SnO_2 (1.498 and 11)
147	63.28	1.468	$CuGa_2O_4$ (1.467 and 40)
145	64.72	1.439	SnO_2 (1.439 and 12)
136	65.94	1.415	SnO_2 (1.416 and 14)
776	68.68	—	220 Palladium solid solution
123	71.38	1.320	SnO_2 (1.322 and 6)
125	78.53	1.217	SnO_2 (1.215 and 9)
640	82.87	—	311 Palladium solid solution
391	87.50	—	222 Palladium solid solution
121	89.63	1.092	SnO_2 (1.092 and 7)
120	90.75	1.082	SnO_2 (1.081 and 8)

In_2O_3 standard at d = 4.130 Å, with a relative intensity of 13% of that for the strongest 222 peak. The latter peak at d = 2.921 Å was missing for the oxide layer, as was the second-strongest 440 peak for the In_2O_3 standard at d = 1.788 Å, which has a relative intensity of 36% of that for the 222 reflection. The d-spacings for the other peaks from the In_2O_3 phase were generally lower than values from the JCPDS, and the peaks at 45.06° and 72.92° were poor matches.

The x-ray diffraction pattern for oxidized air-abraded Legacy in Fig. 4 was dramatically different from that for the oxidized, polished and etched alloy. The oxide layer consisted of β-Ga_2O_3 and PdO. The matches for all the peaks in Fig. 4 obtained with the Philips diffractometer to the d-spacings in the β-Ga_2O_3 JCPDS standard were excellent, as shown in Table 4, with differences not exceeding 0.01 Å, except for the peak at 43.43° where the discrepancy was 0.02 Å. The peaks at 33.69° and 33.91° matched the d-spacings for PdO within 0.01 Å. The presence at 52.61° of the normally very weak peak from the JCPDS where d = 1.744 Å indicated that β-Ga_2O_3 has substantial preferred orientation in oxidized air-abraded Legacy, and this was supported by comparing the relative intensities for other peaks in Fig. 4.

Fig. 5 presents the x-ray diffraction pattern for the oxidized, polished and etched 75Pd-6Ga–6Au-6Ag-6.5In alloy Protocol. All of the peaks for the oxide layer have been indexed to bcc In_2O_3 and β-Ga_2O_3, other than the small peak at approximately 36.4° which does not match peaks for $PdO \cdot xH_2O$ and PdO. It was concluded that α-Ga_2O_3 was not present, since the four strongest peaks for the JCPDS standard were not observed. Further comparisons of the peak positions in Fig. 5 with the JCPDS indicated that none of the silver and palladium oxides were present, nor were any of the $(Ga,In)_2O_3$, β-$GaInO_3$, $AgGaO_2$, and $AgInO_2$ mixed oxides. As with oxidized Legacy, the In_2O_3 phase has extremely high preferred orientation, with the 211 peak at 22.10° (d = 4.019 Å) having a maximum intensity of 2,370 cps. For comparison, the maximum intensities of the 111 peak at 39.80° and the 200 peak at 46.28° for the palladium solid solution of the alloy substrate were 4,664 cps and 1,873 cps, respectively. Also as with oxidized Legacy, the d-spacings for the In_2O_3 phase were generally less than those from the JCPDS. There were poor matches for the 321 peak at 32.90°, the 332 peak at 41.47°, and the 622 peak at 60.29°, which is nearly coincident with a peak for β-Ga_2O_3. In all but one case, the d-spacings corresponding to the observed peaks for the β-Ga_2O_3 phase in the oxide layer were within 0.01 Å of the values for the JCPDS. The exception was the β-Ga_2O_3 peak at 23.81° (d = 3.734 Å), where the difference of 0.05 Å with the JCPDS is attributed to the overlapping shoulder of the 211 In_2O_3 peak. The relatively high intensity of the peak at 23.81° indicates some preferred orientation for the β-Ga_2O_3 phase in the oxide layer, since this is a weak peak for the standard with a relative intensity of only 2% of that for the strongest peak at d = 2.823 Å (31.67°). Further indication of preferred orientation is the strong β-Ga_2O_3 peak at 72.16°, where the corresponding peak in the standard has a relative intensity of only 5% of that for the strongest peak.

The x-ray diffraction pattern for oxidized air-abraded Protocol in Fig. 6 indicates that the oxide layer consisted of β-Ga_2O_3 and PdO; no peaks for In_2O_3 were detected. The peak positions obtained with the Philips diffractometer and their interpretation have been summarized in Table 5. While the general compositions of the oxide layers appeared to be very similar for both Pd-Ga alloys, comparison of Figs. 4 and 6 indicated the relative intensities of the oxide peaks were stronger for Protocol. The agreement between the d-spacings of the peaks for β-Ga_2O_3 in the oxide layer and the corresponding JCPDS peaks was within 0.01 Å, except for the peaks at 31.88° and 43.46° where the agreement was within 0.02 Å; a similar result was found with the latter peak for Legacy. The presence at 52.64° of the normally very weak peak for the standard indicated (as for Legacy) that the β-Ga_2O_3 has preferred orientation, which is again supported by comparisons of the relative intensities of other peaks. The d-spacings for the peaks assigned to PdO in Fig. 6 matched the values in the standard to within 0.015 Å.

The average lattice parameters of the palladium solid solution matrix obtained by the Nelson-Riley analysis of the

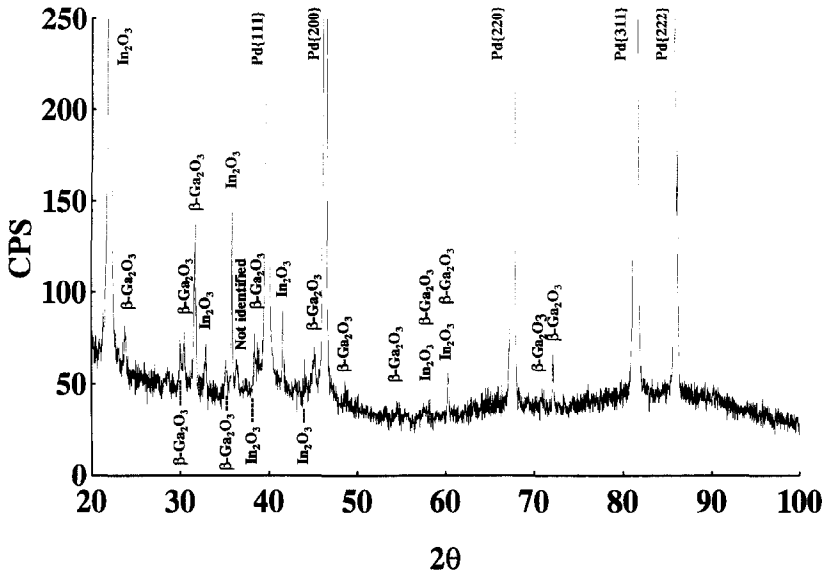

Fig. 5. **X-ray diffraction pattern obtained with the Scintag PAD-V diffractometer for oxidized, polished and etched Pd-Ga alloy Protocol.**

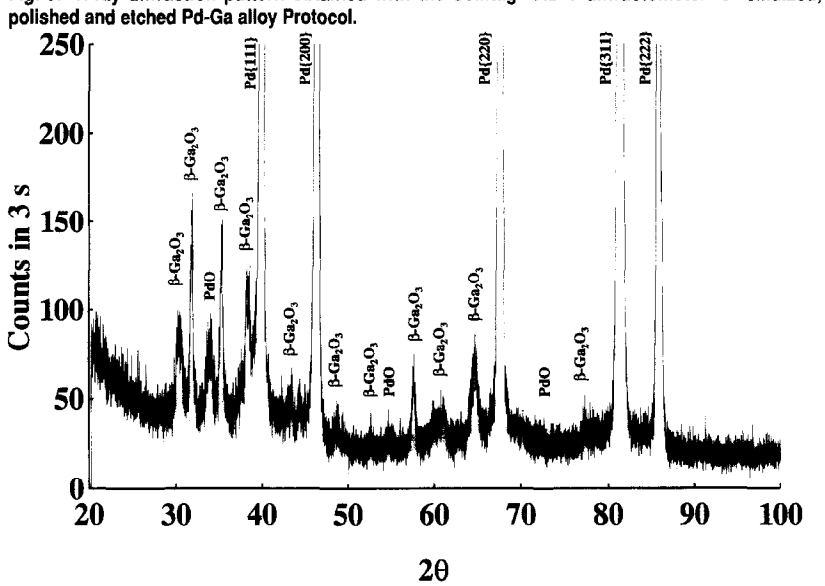

Fig. 6. **X-ray diffraction pattern obtained with the Philips diffractometer for oxidized air-abraded Pd-Ga alloy Protocol.**

data from the three diffractometers for the oxidized alloy substrates (two surface conditions) are given in Table 6 and compared to values obtained for the as-cast alloys (Brantley *et al.,* 1995). The agreement within 0.01 Å of the values of lattice parameter for the as-cast and oxidized conditions of three alloys is the same as that found in the previous study for repeated measurements and duplicate specimens of each as-cast alloy. Hence, within the precision of the present XRD measurements, the lattice parameter of the palladium solid solution for these alloys was minimally changed by oxidation and the surface preparation procedure. The difference of 0.03 Å between lattice parameters of the palladium solid solution for as-cast and oxidized Liberty is attributed to the relatively thick oxide layer on this alloy.

DISCUSSION

The complexity of the oxide layers on representative Pd-Cu-Ga alloys subjected to each manufacturer's recommended oxidation procedure is much greater than previously reported. Using XRD, Hautaniemi *et al.* (1990) identified $CuGa_2O_4$ on an oxidized Pd-Cu-Ga alloy with a composition nearly identical to that of Spartan Plus, whereas Bagby *et al.* (1990) identified both SnO_2 and $CuGa_2O_4$ in the oxidized layer on a Pd-Cu-Ga–Sn alloy with a composition somewhat similar to Liberty. In this study, comparison of the XRD peak positions with the JCPDS indicated that perhaps four phases were present in the oxide layer on oxidized, polished and etched Spartan Plus ($CuGa_2O_4$, β-Ga_2O_3, Cu_2O, and $PdO{\cdot}xH_2O$), whereas five phases may be present in the oxide layer on oxidized, polished and etched Liberty (SnO_2, $CuGa_2O_4$, Cu_2O, and perhaps β-Ga_2O_3 and $PdO{\cdot}xH_2O$). When air-abraded specimens of these Pd-Cu-Ga alloys were oxidized, β-Ga_2O_3 was not present in the oxide layer. The excellent agreement within generally 0.01 Å of the d-spacings for the peaks from the two oxidized Pd-Cu-Ga alloys with corresponding positions for the pure oxide JCPDS standards not only validated the accuracy of the present XRD analyses, but suggested that the oxide phases in the oxide layers on the two Pd-Cu-Ga alloys had relatively little substitutional solid solution incorporation of other cation species.

As previously noted, the presence of α-Ga_2O_3 in the oxide layer on oxidized, polished and etched Liberty cannot be ruled out in principle, because the strongest peaks for this phase coincide with peaks for $CuGa_2O_4$ and SnO_2. Kohn *et al.* (1957) pointed out that striking analogies occur between the oxides of aluminum and gallium, and referred to β-Ga_2O_3 as the high-temperature form of gallium oxide (gallia). Geller (1960) subsequently emphasized that β-Ga_2O_3 is actually the thermodynamically stable form of gallium oxide at room temperature; earlier research by Foster and Stumpf (1951) showed that, while α-Ga_2O_3 forms at lower temperatures than does β-Ga_2O_3, the α-phase is metastable. Hence, the absence of α-Ga_2O_3 in the oxide layer on Liberty is plausible.

The crystal structures of the oxide phases on the oxidized Pd-Cu-Ga alloys are as follows: $CuGa_2O_4$ (cubic spinel structure); β-Ga_2O_3 (monoclinic, which thereby has a very large number of XRD peaks); SnO_2 (tetragonal); Cu_2O (cubic); possibly $PdO{\cdot}xH_2O$ (tetragonal) and PdO (tetragonal) are also present. The lattice parameters from the JCPDS for the pure oxides are provided in Table 7. The crystal structure of the rhombohedral (hexagonal) α-Ga_2O_3 phase, which is isostructural with α-Al_2O_3, has been discussed by Marezio and Remeika (1967).

The much simpler compositions of the oxide layers on the Pd-Ga alloys, Legacy and Protocol, result from the fewer elements in these alloys that form stable room-temperature oxides compared to the two Pd-Cu-Ga alloys studied. Only In_2O_3 was detected on oxidized, polished and etched Legacy, whereas both In_2O_3 and β-Ga_2O_3 were detected on oxidized, polished and etched Protocol. In contrast, when both as-cast Pd-Ga alloys were air-abraded (instead of being polished and etched) and oxidized, the oxide layers contained β-Ga_2O_3 and palladium oxide(s); no In_2O_3 was detected in the oxide layer on either alloy. The matches of the d-spacings to the JCPDS standard were generally within 0.01 Å for PdO, and XPS

TABLE 3 SUMMARY OF OXIDE X-RAY DIFFRACTION PEAKS FROM OXIDIZED, POLISHED AND ETCHED LEGACY

1,947	22.04	4.030	bcc In_2O_3 (4.130 and 13)
185	36.14	2.483	bcc In_2O_3 (2.529 and 33)
122	42.08	2.146	bcc In_2O_3 (2.157 and 6)
75	44.12	2.051	bcc In_2O_3 (2.066 and 1)
65	45.06 (avg.)	2.013	bcc In_2O_3 (1.984 and 10)
61	60.89	1.520	bcc In_2O_3 (1.525 and 24)
72	72.92	1.296	bcc In_2O_3 (1.352 and 2)

TABLE 4 SUMMARY OF X-RAY DIFFRACTION PEAKS FOR OXIDIZED AIR-ABRADED LEGACY

73	29.98	2.979	β-Ga_2O_3 (2.971 and 54)
68	30.23	2.954	β-Ga_2O_3 (2.945 and 49)
65	30.36	2.941	β-Ga_2O_3 (2.934 and 57)
79	31.82	2.810	β-Ga_2O_3 (2.823 and 100)
105	33.69	2.658	β-Ga_2O_3 (2.676 and 17) PdO (2.669 and 22)
108	33.91	2.642	PdO (2.647 and 100)
94	35.19	2.548	β-Ga_2O_3 (2.550 and 68)
105	38.46	2.338	β-Ga_2O_3 (2.344 and 38)
3,650	40.17	—	111 Palladium solid solution
75	43.43	2.082	β-Ga_2O_3 (2.101 and 10)
1,001	46.56	—	200 Palladium solid solution
40	52.61	1.738	β-Ga_2O_3 (1.744 and 1) Indicates preferred orientation
41	54.26	1.689	β-Ga_2O_3 (1.685 and 4) β-Ga_2O_3 (1.682 and 4) PdO (1.676 and 20)
54	57.62	1.598	β-Ga_2O_3 (1.600 and 18)
46	60.83	1.521	β-Ga_2O_3 (1.520 and 18)
52	64.65	1.441	β-Ga_2O_3 (1.453 and 16) β-Ga_2O_3 (1.446 and 14) β-Ga_2O_3 (1.442 and 46)
764	68.14	—	220 Palladium solid solution
575	81.89	—	311 Palladium solid solution
269	86.67	—	222 Palladium solid solution

studies are in progress to confirm the oxide species identified by XRD. While the strongest peak for PdO_2 (standard 34-1101) nearly coincides with a peak for PdO, information provided by the JCPDS indicates that PdO_2 is unstable and decomposes at room temperature. The lattice parameter for the bcc In_2O_3 JCPDS standard is also provided in Table 7.

For both oxidized, polished and etched Pd-Ga alloys, the lattice parameter of the In_2O_3 phase was less than that for the JCPDS standard, which may be due to substitution of smaller Ga^{+3} ions (Kingery *et al.*, 1976) for some In^{+3} ions. The normal room-temperature form of In_2O_3 has a bcc (thallium oxide-type) structure with a lattice parameter of 10.117 Å (Roth, 1957) and 16 molecules per unit cell (Marezio, 1966). It is likely that some special orientation relationship (favored by the relatively smooth and low-stress surface condition of the polished and etched alloys) exists between the crystal structure of In_2O_3 and the face-centered cubic structure of the palladium solid solution matrix for the Pd-Ga alloys, yielding a low-energy interface with preferred orientation of the oxide. Because of the roughened microtopography and substantial internal stresses, this orientation relationship does not exist for the oxidized air-abraded specimens, where the principal phase in the oxide layer was β-Ga_2O_3.

The same preferred orientation of the In_2O_3 phase appeared to exist in the oxide layers on both oxidized, polished and etched Pd-Ga alloys, where three of the strongest six peaks for the In_2O_3 JCPDS standard were missing: the strongest 222 reflection and the 440 and 431 reflections. However, despite the extremely high degree of preferred orientation for the In_2O_3 phase on oxidized, polished and etched Legacy and Protocol, there was essentially no change in the lattice parameter of the underlying palladium solid solution matrix (Table 1), which only has a small amount of preferred orientation for these two as-cast alloys (Brantley *et al.*, 1995). This suggests that any strong metal-oxide interfacial bonds that would create substantial elastic strain in the oxidized layer must have a largely random orientation for the In_2O_3 phase.

For oxidized air-abraded Legacy and Protocol, the presence of the normally very weak peak (d = 1.744 Å) at approximately 52.6° in Figs. 4 and 6, respectively, indicated that the β-Ga_2O_3 phase in the oxide layer had preferred orientation. Similarly, for oxidized air-abraded Liberty, the presence of the normally very weak peak (d = 2.309 Å) at approximately 39.2° in Fig. 3 indicated that the SnO_2 phase in the oxide layer had preferred orientation. (Since none of the x-ray diffractometers used in this study were equipped with a θ-compensating slit, only the foregoing comments about preferred orientation of oxide species were deemed appropriate.) Because of the preferred orientation of these oxide phases, the average crystal sizes cannot be determined from the Scherrer formula (Cullity, 1978), using the breadth of the strongest peaks at half-maximum intensity. Nonetheless, from the strongest peaks for the oxide species in Figs. 1 - 6, it is estimated that the crystal sizes were smaller than approximately 0.5 μm.

It should be noted that the present XRD identifications of phases in the oxide layers on the four high-palladium alloys are consistent with previous SEM/EDS analyses of the near-surface regions of the cast and air-abraded alloys after heat treatment simulating the full firing cycles for Vita VMK porcelain (Brantley *et al.*, 1993). For heat-treated Spartan (with a composition very similar to Spartan Plus), submicron oxide particles with dimensions too small for EDS analyses were embedded in the palladium solid solution matrix, and there were increased concentrations of Ga and Cu

90	30.15	2.962	β-Ga_2O_3 (2.971 and 54)
104	30.23	2.954	β-Ga_2O_3 (2.945 and 49)
99	30.48	2.930	β-Ga_2O_3 (2.934 and 57)
167	31.88	2.805	β-Ga_2O_3 (2.823 and 100)
98	34.04	2.632	PdO (2.647 and 100)
151	35.35	2.537	β-Ga_2O_3 (2.550 and 68)
127	38.55	2.334	β-Ga_2O_3 (2.344 and 38)
6,539	39.94	—	111 Palladium solid solution
67	43.46	2.081	β-Ga_2O_3 (2.101 and 10)
2,283	46.40	—	200 Palladium solid solution
49	48.70	1.868	β-Ga_2O_3 (1.872 and 16)
42	52.64	1.737	β-Ga_2O_3 (1.744 and 1) Indicates preferred orientation
44	54.69	1.677	PdO (1.676 and 20)
75	57.66	1.597	β-Ga_2O_3 (1.600 and 18)
55	60.78	1.523	β-Ga_2O_3 (1.520 and 18)
86	64.76	1.438	β-Ga_2O_3 (1.442 and 46)
1,445	67.67	—	220 Palladium solid solution
40	72.69	1.300	PdO (1.323 and 15)
52	77.33	1.233	β-Ga_2O_3 (1.226 and 2)
1,158	81.41	—	311 Palladium solid solution
468	85.91	—	222 Palladium solid solution

Spartan Plus	3.85	3.86
Liberty	3.89	3.86
Legacy	3.89	3.89
Protocol	3.93	3.92

compared to the bulk matrix. For heat-treated Liberty, submicron particles were also embedded in the palladium solid solution grains, and there were increased concentrations of near-surface Ga, Cu and Sn compared to the bulk matrix; massive grain boundary deposits were tentatively identified as Ga_2O_3. After heat treatment, both Protocol and Legacy also exhibited grain boundary deposits that were tentatively identified as Ga_2O_3.

The role of the decomposition of PdO at elevated temperatures for bubble formation at the interface between dental porcelain and high-palladium alloys has been discussed (Volpe and Cadoff, 1993; Papazoglou *et al.*, 1996). It is conjectured that the time period in the present study for oxidation of the high-palladium alloys was insufficient for complete decomposition of PdO, compared to the longer time periods required for the complete porcelain firing cycles. The conditions for the formation and decomposition of both PdO and PdO·xH_2O are important areas for further investigation. It should also be noted that, in contrast to XRD, XPS analyses are not hindered by the effects of preferred orientation and crystal size (Barr, 1994).

Future research will employ XRD to determine changes in the oxide layers on these high-palladium alloys after complete porcelain firing cycles. Ideally, the changes in the composition of the oxide layer should be investigated with a series of model high-palladium alloys (and perhaps also with variations of the surface preparation techniques) in the manner that Ohno *et al.* (1983) did for gold alloys containing varying amounts of In and Sn. Moreover, direct measurement of the oxide adherence (Mackert *et al.*, 1988) for model high-palladium alloys may provide insight into the development of new compositions with improved metal-ceramic bonding.

ACKNOWLEDGMENTS

Support for this investigation was received from Research Grant DE10147 from the National Institute of Dental Research, Bethesda, MD. The authors wish to thank Professor Rodney J. Tettenhorst, Department of Geological Sciences, for the use of his diffractometer.

Received December 8, 1995 / Accepted June 25, 1996

Address correspondence or reprint requests to:
William A. Brantley
Section of Restorative Dentistry, Prosthodontics and Endodontics
College of Dentistry
The Ohio State University
305 West 12th Avenue
Columbus, OH 43210-1241 USA
Tel: (614) 292-0773
FAX: (614) 292-9422

REFERENCES

Bagby M, Marshall SJ, Marshall Jr GW (1990). Effects of porcelain application procedures on two noble alloys. *J Appl Biomater* 1:31-37.

Barr TL (1994). Modern ESCA. Boca Raton, FL: CRC Press, 5-29.

Brantley WA, Cai Z, Carr AB, Mitchell JC (1993). Metallurgical structures of as-cast and heat-treated high-palladium dental alloys. *Cells Mater* 3:103-114.

TABLE 1. LATTICE PARAMETERS FOR THE PURE OXIDE SPECIES POSSIBLE BONDING TO THE PHASES IN THE OXIDE LAYERS ON THE HIGH-PALLADIUM ALLOYS

$CuGa_2O_4$	Cubic (Spinel)	a = 8.298 Å	26-514
SnO_2	Tetragonal	a = 4.7382 Å c = 3.1871 Å	41-1445
Cu_2O	Cubic	a = 4.2696 Å	5-667
β-Ga_2O_3	Monoclinic	a = 12.236 Å b = 3.0399 Å c = 5.8120 Å β = 103.76°	41-1103
$PdO \cdot xH_2O$*	Tetragonal	a = 2.994 Å c = 5.403 Å	9-254
PdO*	Tetragonal	a = 3.0456 Å c = 5.3387 Å	41-1107
In_2O_3	Body-centered cubic (Thallium oxide-type)	a = 10.118 Å	6-416

Brantley WA, Cai Z, Foreman DW, Mitchell JC, Papazoglou E, Carr AB (1995). X-ray diffraction studies of as-cast high-palladium alloys. *Dent Mater* 11:154-160.

Carr AB, Brantley WA (1991). New high-palladium casting alloys: Part 1. Overview and initial studies. *Int J Prosthodont* 4:265-275.

Cascone PJ (1983). Oxide formation on palladium alloys and its effect on porcelain adherence. *J Dent Res* 62:255, Abstr. No. 772.

Craig RG, editor (1993). Restorative Dental Materials. 9th ed. St. Louis: Mosby, 491-499.

Cullity BD (1978). Elements of X-ray Diffraction. 2nd ed. Reading, MA: Addison-Wesley, 99-102, 356-357.

Foster LM, Stumpf HC (1951). Analogies in the gallia and alumina systems. The preparation and properties of some low-alkali gallates. *J Am Chem Soc* 73:1590-1595.

Geller S (1960). Crystal structure of β-Ga_2O_3. *J Chem Phys* 33:676-684.

Hautaniemi JA, Juhanoja JT, Suoninen EJ, Yli-Urpo AUO (1990). Oxidation of four palladium-rich ceramic fusing alloys. *Biomater* 11:62-72.

Kingery WD, Bowen HK, Uhlmann DR (1976). Introduction to Ceramics. 2nd ed. New York: Wiley, 56-61.

Kohn JA, Katz G, Broder JD (1957). Characterization of β-Ga_2O_3 and its alumina isomorph, θ-Al_2O_3. *Am Mineral* 42:398-407.

Mackert Jr JR, Ringle RD, Fairhurst CW (1983). High-temperature behavior of a Pd-Ag alloy for porcelain. *J Dent Res* 62:1229-1235.

Mackert Jr JR, Ringle RD, Parry EE, Evans AL, Fairhurst CW (1988). The relationship between oxide adherence and porcelain-metal bonding. *J Dent Res* 67:474-478.

Marezio M (1966). Refinement of the crystal structure of In_2O_3 at two wavelengths. *Acta Crystallogr* 20:723-728.

Marezio M, Remeika JP (1967). Bond lengths in the α-Ga_2O_3 structure and the high-pressure phase of $Ga_{3-x}Fe_xO_3$. *J Chem Phys* 46:1862-1865.

Mezger PR, Stols ALH, Vrijhoef MMA, Greener EH (1988). Metallurgical aspects of high-palladium alloys. *J Dent Res* 67:1307-1311.

Ohno H, Kanzawa Y, Kawashima I, Shiokawa N (1983). Structure of high-temperature oxidation zones of gold alloys for metal-porcelain bonding containing small amounts of In and Sn. *J Dent Res* 62:774-779.

Papazoglou E, Brantley WA, Carr AB, Johnston WM (1993). Porcelain adherence to high-palladium alloys. *J Prosthet Dent* 70:386-394.

Papazoglou E, Brantley WA, Mitchell JC, Cai Z, Carr AB (1996). New high-palladium casting alloys: Studies of the interface with porcelain. *Int J Prosthodont* 9:315-322.

Philips RW (1991). Skinner's Science of Dental Materials. 9th ed. Philadelphia: Saunders, 521-523.

Ringle RD, Mackert Jr JR, Fairhurst CW (1983). An x-ray spectrometric technique for measuring porcelain-metal adherence. *J Dent Res* 62:933-936.

Roth RS (1957). Classification of perovskite and other ABO_3-type compounds. *J Res Natl Bur Std* 58:75-88.

van der Zel JM (1989). High-temperature behavior of palladium-based dental alloys. Doctoral dissertation, University of Amsterdam.

Volpe C, Cadoff I (1993). Oxidation kinetics of palladium alloyed with gallium, indium and silver. *J Dent Res* 72:305, Abstr. No. 1612.